Comparative Theoretical and Experimental Study of the Radiation-Induced Decomposition of Glycine

R. G. Wilks,*,† J. B. MacNaughton,† H.-B. Kraatz,‡ T. Regier,§ R. I. R. Blyth,§ and A. Moewes†

Department of Physics and Engineering Physics, University of Saskatchewan, 116 Science Place, Saskatoon, Saskatchewan, S7N 5E2, Canada, Department of Chemistry, The University of Western Ontario, 1151 Richmond Street, London, Ontario, N6A 5B7, Canada, Canadian Light Source Inc., University of Saskatchewan, 101 Perimeter Road, Saskatoon, Saskatchewan, S7N 0X4, Canada

Received: January 27, 2009; Revised Manuscript Received: March 19, 2009

The radiation-induced decomposition of glycine is studied using a combination of near-edge X-ray absorption fine structure (NEXAFS) measurements and DFT calculations. The measured spectra show strong dose- or time-dependent effects consistent with a complex, multistep decomposition. Principal component analysis was used to determine the number of distinct molecules that were needed to explain the observed changes in the measured spectra, and the emerging absorption features are assigned to various product molecules through comparison with simulated spectra of several model compounds. It is clear from the experiment that the major effect of soft X-ray irradiation is the fragmentation of the molecule, primarily at the carbonyl sites. Peptide formation is shown to occur under irradiation; a condensation reaction initiated by the removal of a carbonyl oxygen is the proposed mechanism. This study utilizes a novel approach to the study of radiation damage that can occur during measurements and suggests that it may be possible to use simulated model spectra to correct for these effects in measured spectra.

1. Introduction

The damage that occurs when amino acids are subjected to intense soft X-ray radiation is a matter of concern to both the medical and physical chemistry communities. Understanding the mechanisms that lead to such damage is vital if methods to avoid or repair such damage are to be developed. There are many synchrotron-based techniques that use soft X-rays to determine structural, electronic, and magnetic properties. However, many systems including large biological molecules such as proteins and DNA are prone to radiation damage, and the effects on the obtained data cannot be neglected. Amino acids are the building blocks of proteins, and their simplicity and availability makes them ideal candidates to study the effects of radiation.

Several EPR-based studies of radical formation in glycine have tackled this topic in the past,[1−6] and the structures and other properties of the radicals have been modeled using DFT with a fair degree of success.[6,7] Electrochemical measurements of amino acids in solution have shown that the main effect of low-energy (i.e., UV) ionizing radiation is the deprotonation of the C_α site,[8] which leads to the production of the radical species that are detected in EPR studies. Zubavichus et al. documented the effects of radiation damage on the NEXAFS spectra of several complex amino acids, employing XPS and mass spectrometry as complementary experimental techniques.[9,10] Several decay mechanisms were proposed, including deprotonation and the removal of carbon dioxide; the importance of these mechanisms is reinforced in the current study. Studies of polymer materials have suggested that the primary mechanism for radiation damage is the removal of the carbonyl.[11,12] It has been found that X-ray spectroscopic techniques are effective probes of the electronic structure of amino acids including glycine.[13−18]

A variety of theoretical techniques have been used in the past to model the measured near-edge soft X-ray absorption spectra of glycine. StoBe DFT[19] was used to model the spectra of glycine adsorbed onto substrates by Nyberg and Hasselström.[20−23] Gordon et al. performed NEXAFS measurements and complementary Hartree−Fock simulations to analyze the effects of the conformation of glycine and glycine peptides on the measured spectra.[14] Plashkevych et al. compared DFT simulations with measurements of glycine near-edge spectra, extending the work to include circular dichroism measurements.[24] In this study, we will present a series of NEXAFS measurements at the C 1s and N 1s edges showing the effects of irradiation on a primarily zwitterionic glycine sample. The identities of the product molecules will be determined through comparison with StoBe-simulated NEXAFS spectra of numerous candidate molecules, and the details of the induced reactions will be discussed.

2. Experimental Details

Glycine powder was purchased from Alfa-Aesar, and was used as delivered in powder form, without further purification. The sample was mounted on the holder by pressing the powder onto a freshly scraped indium foil surface. The soft X-ray absorption spectra of the C and N 1s edges were measured at the undulator-based spherical grating monochromator (SGM) beamline at the Canadian Light Source (CLS) synchrotron at the University of Saskatchewan. The monochromator resolution was approximately 100 meV, similar to the energy step size used to record the spectra (100 meV for the C spectra, 200 meV for N). The absorption spectra were measured in both total

* To whom correspondence should be addressed. E-mail: regan.wilks@usask.ca.
† Department of Physics and Engineering Physics, University of Saskatchewan.
‡ Department of Chemistry, The University of Western Ontario.
§ Canadian Light Source Inc., University of Saskatchewan.

10.1021/jp900794v CCC: $40.75 © 2009 American Chemical Society
Published on Web 04/10/2009

electron yield (TEY), in which absorption is monitored via measurement of the sample current, and total fluorescence yield (TFY), in which absorption is monitored through detection of photons produced through relaxation of the excited states. The incoming photon flux was measured simultaneously with the absorption spectra on a highly transparent gold mesh and subsequently used for normalization of the data. A new layer of gold was sputtered onto the mesh immediately prior to our measurements to minimize the effects of contamination on the normalization procedure. No resonance absorption peaks were seen upon examination of the measured mesh current spectrum, indicating that the mesh itself was not contaminated during the performance of the experiment. However, large dips in the intensity of the current unavoidably occur at 284.2 and 291.0 eV, which can sometimes lead to spectral artifacts. Although we have no reason to believe that there are any normalization problems at the C edge in the current experiment, the possibility of spectral distortion due to very low photon flux in the region around 284.4 eV corresponding to features in the C 1s NEXAFS spectra cannot be entirely dismissed. By examining the raw electron yield spectra, however, it was clear that a signal associated with the material being measured did indeed occur at the energy of feature *a*′, and so we carry on under the assumption that any effects associated with normalization would have no significant impact on the conclusions reached in this study.

This experiment involved using synchrotron radiation to irradiate the glycine sample and monitor the damage induced by measuring element-selective absorption spectra. The carbon NEXAFS spectra were collected at ∼180 mA ring current and each scan took 416 s. The nitrogen NEXAFS spectra were collected at ∼140 mA and each scan took 220 s. The π^*-region-only scans for the N edge was measured at ∼130 mA and 49 s. A new spot on the sample was measured for each set of measurements; and all of the spectra for a given edge were measured successively, except where otherwise noted. This procedure allowed the effects of radiation damage to be studied as a function of time and radiation dose. Unfortunately, several factors make it difficult to estimate the radiation dose, particularly the noncontinuous intensity of the X-rays: when the excitation energy is stepped, the undulator and monochromator do not move in a synchronized manner, leading to a temporary drop in intensity. A very rough estimate suggests that each scan delivers a radiation dose of 200−400 Gy, although it should be noted that for the purposes of this manuscript, several scans, particularly in the latter stages of the experiment where the changes occurred slowly and predictably, were omitted from the plots. The scans were repeated until a saturation of the damage effects was observed, with the last spectrum in each series measured after the monochromator slits had been opened for five minutes, delivering an extremely large radiation dose to the material.

For the StoBe calculations, triple-ζ plus valence polarization (TZVP) Huzinaga basis sets[25] were used to describe the orbitals; A5 auxiliary basis sets, derived from the TZVP sets, were also used in the calculation.[26] The orbitals of the atom undergoing excitation were represented by a iii_iglo basis set,[26,27] and a large, diffuse auxiliary basis set was added at this location to model the unoccupied orbitals. The oscillator strengths for transitions from the core level to the unoccupied excited-state orbitals were calculated; for comparison with the measured spectra the oscillator strengths were convoluted with Gaussian functions of varying widths. The C spectra had line widths of 0.6 eV (fwhm) up to the ionization potential and then linearly increasing to 4.5 eV (fwhm) over the next 10 eV; the N spectra had line widths of 0.6 eV (fwhm) up to the ionization potential and then linearly increasing to 5.5 eV (fwhm) over the next 10 eV. The geometry of the zwitterionic α-glycine was taken from the experimental findings of Langan et al.;[28] all other geometries were optimized with StoBe DFT.

To determine the most accurate possible energy calibration of the calculated spectra, several additional calculations were required. As was alluded to by Cavalleri et al.,[29] an improved description of the relaxation of the excited states can be obtained by determining the difference in energy between the molecule's ground state and the first core-excited state. For the N-edge simulations, this procedure involved two additional calculations: one in which no core hole was present, and one which contained a completely unoccupied 1s core hole−as opposed to the half-occupied core level used in the transition state approximation− and an extra electron in the lowest unoccupied molecular orbital (LUMO). The energy required to cause the transition between ground and excited states is then determined by finding the difference in total energies−minimized in the self-consistent field procedure−of the two states and shifting the spectra calculated using the transition-state approximation such that the lowest-energy transition occurs at this energy. Employment of this approach leads to a vast improvement in the calculated energy axes, improving the agreement between the measured and simulated results and providing support for the use of these simulations in the production of model spectra for use in the assignment of spectral features.

A similar approach was used in the modeling of the C 1s absorption spectra but in this case an extra degree of complexity was introduced as a result of the presence of multiple non-equivalent C sites in the majority of the molecules being modeled. In these cases, each site required a separate set of calculations, and the differences in relaxation effects led to different energy shifts being required for each site, leading to, in some cases, a significant modification of the spectral line shape.

The measured spectra were calibrated by comparing them to the spectra of reference samples that were measured with the same monochromator settings. Because absolute energy calibration is not possible, it was assumed that the measured spectra were correct, and a slight, uniform shift was applied to all simulated spectra (preserving the relative calculation determined using the method described in the preceding paragraphs) to bring them in line with the measurements. The simulated N spectra were shifted 1.9 eV to higher energy so that the center of the broad resonance in the spectrum of zwitterionic glycine occurred at 407.5 eV. The C spectra were shifted 2.1 eV to higher energy so that the main carbonyl feature appeared at 290.0 eV.

Principal component analysis (PCA) was performed using the *exafspak* software[30] to determine the number of molecules that contributed spectral signatures to the measured spectra. The input to the PCA routine was the sets of measured data taken at each edge, and the output is a series of eigenfunctions that are needed to reconstruct each spectrum in the data set. By systematically testing whether an eigenfunction is necessary to the reconstruction, the minimum number of components in the data set can be determined. Although the eigenfunctions do not resemble the individual spectral components, the number of necessary eigenfunctions is identical to the number of individual contributing components.

3. Results and Discussion

Consecutive measurements of the nitrogen near-edge absorption spectrum of glycine show a clear evolution as a function

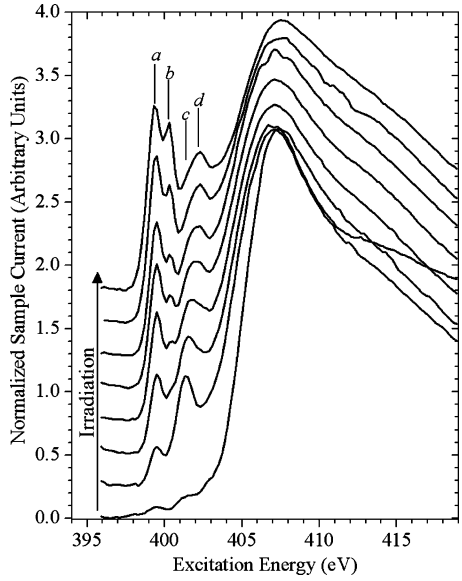

Figure 1. Nitrogen near-edge absorption spectra of glycine, showing the evolution of the spectral features as a function of irradiation. The bottom spectrum represents the least exposure to soft X-rays.

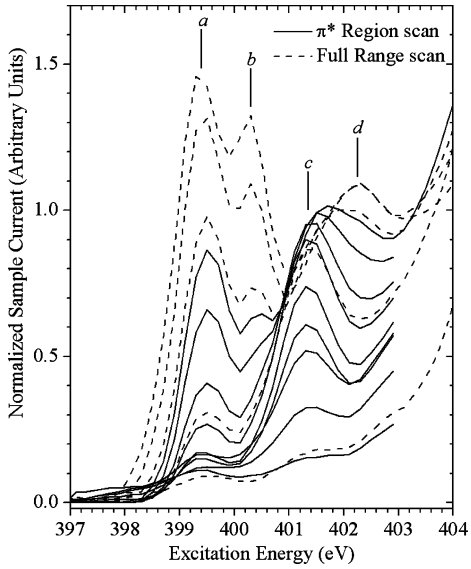

Figure 2. N π^* region near-edge absorption spectra showing radiation damage. The dashed lines are reproduced from the full-range spectra of Figure 1.

of radiation dose, particularly in the π^* region of the spectra. Surprisingly, the most significant changes are seen when the exposure time is relatively low, between the first and second spectra. This dramatic change is clearly visible in Figure 1. The N NEXAFS spectrum should not exhibit any π^* features in the 400−403 eV range due to the absence of any N double bonding or peptide bonding. In light of the significant damage that occurs almost immediately upon irradiation, it can be assumed that this is the source of the minor features seen in this region of the first measured spectrum.

To confirm this assumption and to better investigate the early stages of the damage processes, a second set of scans of only the π^* region from 398−404 eV was performed; these scans are combined with the full-range scans in Figure 2. As expected, the π^* features that were present at the beginning of the scans evolve upon irradiation. It is also clear from the changes in the peak ratios that there are time- or dose-dependent factors in the

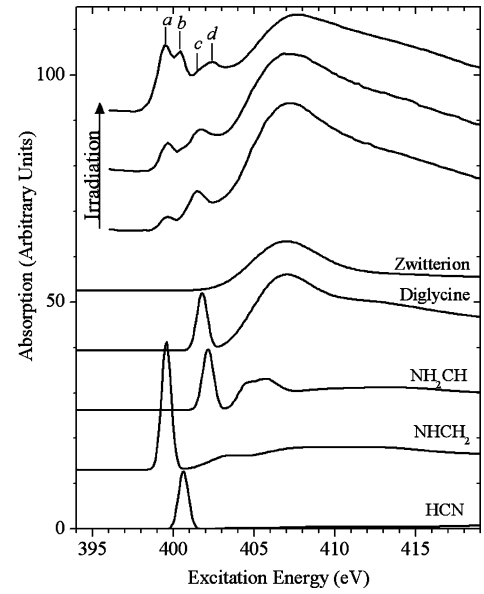

Figure 3. Measured N 1s NEXAFS spectra of glycine showing increasing degrees of radiation damage compared to the StoBe DFT simulations of the spectra of zwitterionic glycine, diglycine, NH_2CH, $NHCH_2$, and HCN (*absorption/5 for display purposes*).

TABLE 1: Proposed Assignments of Main Spectral Features Observed in N 1s NEXAFS Spectra of Irradiated Glycine, Based on Models Produced by StoBe DFT Calculations

feature	energy [eV] (calculated[a])	chemical group (model compound)
a	399.5 (399.5)	imine ($NHCH_2$)
b	400.5 (400.6)	nitrile (HCN)
c	401.3 (401.6)	peptide (diglycine)
d	402.3 (402.1)	amine-surface, reactive (NH_2CH)

[a] After 0.9 eV shift to higher energy.

radiation damage process, and that several product molecules are involved.

The PCA of the N edge spectra indicate that there are five separate contributions to the data set, suggesting that four relatively stable product molecules are present in addition to the undamaged glycine zwitterion. The pre-edge regions of the N absorption spectra consist of four peaks, the intensities of which vary independently over the course of the experiment, suggesting that each can be used to identify a separate component. In Figures 1 and 2, peak *c* appears to migrate to higher energy as a function of irradiation, from 401.3 to 402.3 eV. This migration is an illusion, however, as close examination of the spectra show that it is in fact caused by the emergence of a competing, higher-energy peak. The proposed assignments of these peaks−as well as the other features appearing in the measured spectra−are based on the comparison with the DFT simulations. Figure 3 shows a representative sample of the measured spectra compared to the simulated spectra of the proposed product molecules, and the peak energies and proposed assignments are summarized in Table 1. Table 2 shows the atom positions that were used in the StoBe DFT simulations. The numbering scheme has been kept consistent throughout, with the origin placed at the N-terminus.

Feature *c* corresponds closely in energy to the characteristic absorption peak of the peptide bond of diglycine.[14] Peptide formation via a condensation reaction is the proposed mechanism. Carbonyl groups have been shown to be very susceptible to radiation damage,[9−12] and it appears that irradiation leads

TABLE 2: Atom Positions Used in DFT Simulation of N and C Edge NEXAFS Spectra

	x (Å)	*y* (Å)	*z* (Å)
Zwitterion			
N1	0.000	0.000	0.000
C1	1.475	0.000	0.000
C2	2.040	1.416	0.000
O1	1.279	2.340	0.360
O2	3.237	1.554	−0.347
Diglycine			
N1	0.000	0.000	0.000
C1	1.492	0.000	0.000
C2	1.806	1.527	0.000
O1	5.406	1.157	0.000
N2	3.078	1.785	0.000
C3	3.881	3.003	0.000
C4	5.370	2.448	0.000
O2	6.282	3.290	0.000
O3	0.782	2.284	0.000
NH_2CH			
N1	0.000	0.000	0.000
C1	1.320	0.000	0.000
$NHCH_2$			
N1	0.000	0.000	0.000
C1	1.279	0.000	0.000
HCN			
N1	0.000	0.000	0.000
C1	1.160	0.000	0.000

directly to the removal of an oxygen ion. Rapid peptide formation through interaction with an adjacent glycine, coupled with the expulsion of H_2O from the sample, would complete the reaction. The absorption spectrum of the N-terminus of the peptide is identical to that of the glycine zwitterion, and so feature *d* reflects the contribution of amide bonds, rather than the contribution of peptides. If only diglycine is formed as a result of irradiation, then this distinction is academic. It is likely that larger peptides—triglycine, and so forth—are formed, and so the distinction becomes important, as the proportion of N sites participating in peptide bonds will increase accordingly. The principal component analysis would not likely be able to distinguish the presence of separate contributions from diglycine and larger peptides, and we assume that larger aggregations are present in the sample. The formation of a diketopiperazine cannot be entirely ruled out, however the simulation of its absorption spectra (not shown) did not suggest that it is present in any significant quantity.

The above assumptions can in fact be generally applied to the comparison of the simulated spectra of the model compounds to the measured data. The N 1s NEXAFS spectra of particular N-containing chemical groups will not be particularly sensitive to the nature of the extended structure to which it is attached; if the energy shift in the characteristic peak position is less than the resolution of the measurement, the presence of multiple closely related structures would not be indicated by the principal component analysis. The set of reaction products proposed here is internally consistent, effectively reproducing all features in the measured N-edge and, as will be discussed in the following sections, C-edge spectra. However, in light of the inherent uncertainty involved, the conclusions will be restricted to the identification of the functional groups present in the sample.

The removal of the entire carbonyl would lead to the expulsion of CO_2 and the formation of $NHCH_2$ and NH_2CH. The StoBe simulations of their absorption spectra produce peaks at 399.5 and at 402.1 eV, respectively, in agreement with the positions of features *a* and *d* in the measured spectrum.

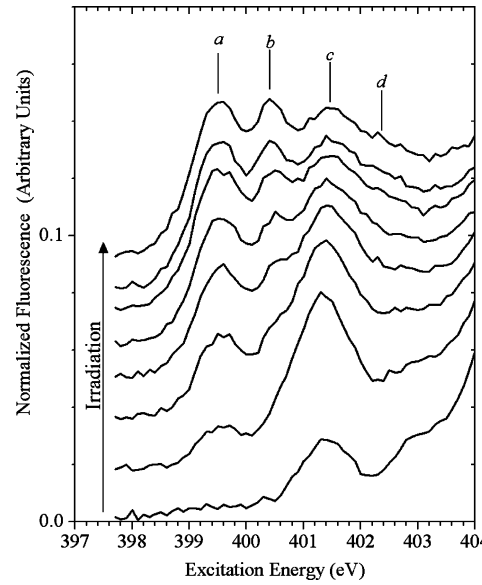

Figure 4. N 1s absorption spectra measured in depth-sensitive TFY mode showing evolution of spectral features associated with increasing radiation dose.

Another possible origin for feature *c* is suggested by previous studies[31,32] in which trapped N_2 gas was found in irradiated materials. We attempted high-resolution scans of the energy region around features *c* and *d* and saw no evidence of vibrational structure that would suggest the presence of trapped N_2 gas.[32] Although we cannot rule out the presence of trapped N_2 gas in the sample, the mechanism for peptide formation above seems to give a much more plausible assignment of the origin of peak *c*.

Fluorescence yield measurements have depth sensitivity on the order of 100 nm at this energy—an order of magnitude larger than that of electron yield measurements—and so the spectra shown in Figure 4 indicate that there is a depth dependence on the composition of the damaged material. Peaks *a* and *d* are particularly suppressed in the fluorescence measurements, suggesting that the NH_2CH and $NHCH_2$ are primarily produced near the surface of the material; this may reflect the relative ease at which CO_2 can be expelled from the surface of the material, leading to decreased opportunity for recombination. The near disappearance of peak *d* in the bulk-sensitive fluorescence yield measurements is consistent with the model of a highly reactive structure derivative isolated on the sample surface under UHV conditions. The TFY spectra indicate that the $NHCH_2$ group is not present in the bulk of the sample in any detectable quantity. The suppression of peak *a* suggests that the imine group, represented by NH_2CH, is also more abundant on the surface than in the bulk, although the contrast is significantly less pronounced.

Some of the changes in peak ratios may be attributable be due to self-absorption of the fluorescence photons but this is unlikely to be the primary cause, as self-absorption more strongly affects intense, sharp resonance absorption features and would not explain the near-disappearance of peak *d*. The relatively late emergence of peak *b*, which is attributed to absorption by HCN, suggests that the nitrile groups may be produced via a secondary reaction involving the breakdown of one of the other products. It is also entirely possible that the peak is due to a more complex nitrile, such as NH_2CN, with a similar N≡C bond length. Although the relative prominence of peak *b* in the fluorescence yield spectra as compared to the

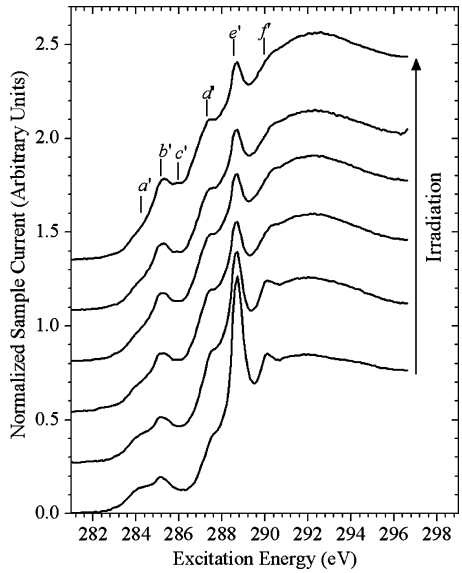

Figure 5. Measured C 1s NEXAFS spectra of glycine. The least-irradiated spectrum is at the bottom, and the most irradiated spectrum is at the top. The background signal has been subtracted, the spectra were normalized to unity at 294 eV, and a horizontal offset has been added for clarity.

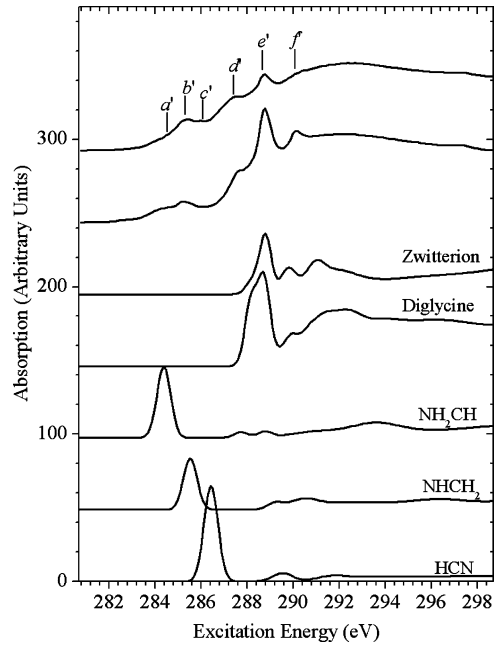

Figure 6. Measured C 1s NEXAFS spectra of damaged glycine (*top two spectra*) compared to the StoBe DFT simulations of the spectra of zwitterionic glycine, diglycine, NH_2CH, $NHCH_2$, and HCN.

electron yield spectra is consistent with the model of a trapped gas, we cannot claim to have unambiguously identified the presence of HCN in the irradiated sample.

The measured C 1s NEXAFS spectra in Figure 5 show the effects of the increasing radiation dose in the evolution of the spectral features. The general trend that was observed in the measurements of the N-edge spectra—that of increasing π^* resonance intensity—is reproduced, although the dynamic behavior at the C-edge is less complex. The decrease in the intensity of feature e' is indicative of the expected[9−12] damage to the carbonyl, providing an indirect confirmation of the conclusions drawn from the N absorption spectra. The combined evidence of the C and N absorption spectra suggest that the removal of all or part of the carbonyl group is the primary damage mechanism under soft X-ray irradiation, regardless of the specific energy of the incoming photons.

The simulated C spectra of the proposed radiation products are shown in Figure 6. The PCA of the C edge spectra was in agreement with the analysis of the N edge spectra, suggesting the presence of five components to the data set. In further agreement with the modeling of the N edge spectra, the simulated C edge spectra predict resonance absorption peaks at energies corresponding to all major features in the measured spectra. There is also evidence of energy dependence in the relative abundance of the products. Compared to the N edge absorption, the intensities of the peaks associated with molecules having deprotonated N sites—especially the completely deprotonated HCN—are suppressed in the C edge spectra. This observation suggests a possible connection between the resonant absorption of photons and the nature of the induced reaction, which would imply that removal of electrons from the bonding orbitals plays a dominant role in the decomposition process. The current methods are not sufficiently quantitative to determine unambiguously whether this is the case, however, and a more directed study of the relationship between resonant excitation and the induced chemical reactions would be required to draw any firm conclusions.

As somewhat of an aside, we feel that it is worthwhile at this point to discuss a matter concerning the calculated C

TABLE 3: Proposed Assignments of Main Spectral Features Observed in C 1s NEXAFS Spectra of Irradiated Glycine, Based on Models Produced by StoBe DFT Calculations

feature	energy [eV] (calculated*)	assignment
a'	284.6 (284.4)	NH_2CH
b'	285.3 (285.5)	$NHCH_2$
c'	286.2 (286.4)	HCN
e'	288.8 (288.8)	glycine zwitterion carbonyl
f'	290.1 (289.9)	glycine zwitterions

* After 2.1 eV shift to higher energy.

absorption spectrum of the glycine zwitterion. Although peak f' is clearly associated with the spectrum of zwitterionic glycine, we must at this point discuss a small degree of uncertainty about the exact origin of the feature. As can be seen from Figure 6, the simulated spectrum of the zwitterion has two features, at 289.8 and 291.0 eV, that have the basic shape of feature f' and are located near it on the energy scale. In our model, it appears that the lower-energy peak in the simulation is the source of this feature but the case could be argued either way. Although it does not have a direct bearing on the conclusions of this study, the point is worth addressing at this point, as the fit to the measured data would be improved by shifting the simulated absorption spectrum of the C_α site of the glycine zwitterion to lower energy by 0.9 eV will cause the higher-energy of the two peaks to align with feature f' and also lead to an increase in the intensity in the region of feature d'. Varying the bond lengths and angles around the C_a site could conceivably cause such a shift in the relative energies of the two C site spectra; however, we did not wish to manipulate our results in this way, choosing rather to use the geometry that was experimentally determined by Langan et al.[28] for the spectral simulations. Also, because of the uncertainty surrounding the nature of d', we have elected to leave it out of Table 3.

As a qualitative test of the numerical models, weighted sums of the individual components were used to reproduce the shape of three representative N absorption spectra; the results are displayed in Figure 7. Because the intensity of the calculated

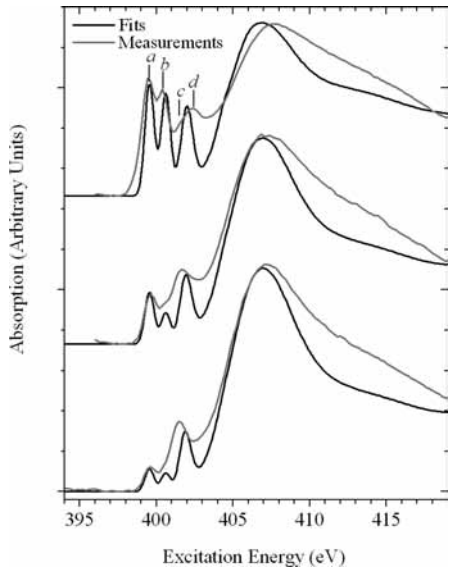

Figure 7. Fits produced by superposition of simulated spectra, compared with measured N edge absorption spectra of glycine.

peaks is strongly dependent on the broadening scheme that is used, it is not possible to make absolute determinations of the relative abundance of each respective material, and so it must be made clear to the reader that the percentages referenced in the following discussion should be viewed as qualitative guides, reflecting no more than the order of magnitude of the relative abundance of any material. Notwithstanding this caveat, however, a few useful observations can be inferred from the fitting procedure. It is clear that, despite the prominence of the resonance absorption features in the near-edge region, the concentrations of several of the various product molecules are very small, considering the large level of energy introduced into a very small portion of the sample. For example, the HCN contributes approximately 4% to the fit made to the topmost spectrum, which had been subjected to an extremely high radiation dose in an attempt to produce a saturation of the effect. HCN concentration (4%) would be a very large concentration, even given the extremely high radiation dose that this region receives, which lends further support to the presence of multiple nitriles that have similar spectra. Furthermore, no relaxation time was allowed between the irradiation and the measurement, and so it is likely that several of the product molecules would dissipate rapidly. Additional stability may be lent to the products because of the fact that they are produced in situ in a very high vacuum environment.

The simulated diglycine spectrum contributes 16% to the fit of the topmost spectrum in Figure 7. It is possible that that may overstate the presence of peptides in the material because, as was previously discussed, it is likely that larger peptides are formed as a result of irradiation. As it is not possible to determine the relative abundance of diglycine, triglycine, and so forth, we have used only diglycine in the analysis.

Both NH_2CH and $NHCH_2$ contribute 20% to the topmost fit in Figure 7. Because of the depth profile of the products that was discussed earlier, this number overestimates the contribution of the NH_2 and NH groups. Assuming that self-absorption does not have a significant effect on the relative intensities of the peaks in Figure 4, a better approximation of their concentrations is on the order of 10%.

4. Discussion and Conclusions

In this study, we have used the N edge NEXAFS spectra to attempt to determine the nature of the products that are produced in irradiated glycine samples. Because of the clear evolution of the spectra as a function of increasing radiation dose and the relatively few possible bonding environments for the N site, we can assign the observed features in the N edge spectra to particular chemical groups with a fair degree of confidence. However, the analysis of the C edge spectra is inherently more ambiguous due to the multiple nonequivalent groups in the majority of the products and to the less spectacular evolution of the measured spectra. We have therefore used the C edge spectra primarily to confirm the conclusions drawn from the analysis of the N edge spectra. The comparison of the simulated spectra of the proposed products provides a self-consistent result with the same molecules used to assign the peaks in both the C and N 1s NEXAS spectra. The proposed set of products is also consistent with the results of the principal component analysis, which suggested that five distinct spectral signatures were present in the measured data sets. The products included in the simulations of the spectra are model compounds that represent general classes of materials.

A large number of possible products were considered as possible contributors to the measured spectrum and were modeled in the same manner as those described above before being ruled because they did not match the measured data. The spectra of several ionic and radical species were modeled and no evidence was found to warrant their inclusion in the proposed model. Because of the highly reactive nature of such compounds, it is unlikely that they could be stable in a solid state in sufficient quantities to be detectable.

This study utilizes soft X-ray absorption spectroscopy to monitor the radiation-induced reactions that occur in solid-state glycine in very high vacuum conditions. By analyzing the evolution of the spectra using a combination of principal component analysis and DFT simulations, a possible model of the damage process in terms of the chemical classes present in the sample is obtained. In agreement with previous studies of the effects of soft X-ray irradiation on organic materials, it is observed that the carbonyl group is highly sensitive to the effects of irradiation, and is largely removed from the material over the course of the experiment. Our results suggest that removal of an oxygen ion from the carbonyl group induces the formation of peptides in the sample. By comparing the surface-sensitive electron yield and the bulk-sensitive fluorescence yield NEXAFS spectra, we conclude that removal of CO_2 from the sample upon irradiation occurs and that it is more likely to occur near the surface of the sample.

Acknowledgment. We gratefully acknowledge support from the Natural Sciences and Engineering Research Council of Canada (NSERC) and the Canada Research Chair program. The research described in this article was performed at the Canadian Light Source, which is supported by NSERC, NRC, CIHR, and the University of Saskatchewan.

References and Notes

(1) Bonazzola, L.; Iacona, C.; Michaut, J.; Roncin, J. *J. Chem. Phys.* **1980**, *73*, 4175.
(2) Hedberg, A.; Ehrenberger, A. *J. Chem. Phys.* **1968**, *48*, 4822.
(3) Morton, J. *J. Am. Chem. Soc.* **1964**, *86*, 2325.
(4) Sagstuen, E.; Sanderud, A.; Hole, E. *Radiat. Res.* **2004**, *162*, 112.
(5) Sanderud, A.; Sagstuen, E. *J. Phys. Chem. B* **1998**, *102*, 9353.
(6) Ban, F.; Gauld, J.; Boyd, R. *J. Phys. Chem. A* **2000**, *104*, 5080.
(7) Pauwels, E.; Van Speybroeck, V.; Waroquier, M. *J. Phys. Chem. A* **2004**, *108*, 11321.
(8) Jonsson, M.; Kraatz, H.-B. *J. Chem. Soc., Perkin Trans.* **1997**, *2*, 2675.
(9) Zubavichus, Y.; Fuchs, O.; Weinhardt, L.; Heske, C.; Umbach, E.; Denlinger, J. D.; Grunze, M. *Radiat. Res.* **2004**, *161*, 346.

(10) Zubavichus, Y.; Zharnikov, M.; Shaporenko, A.; Fuchs, O.; Weinhardt, L.; Heske, C.; Umbach, E.; Denlinger, J. D.; Grunze, M. *J. Phys. Chem. A* **2004**, *108*, 4557.

(11) Wang, J.; Morin C.; Li, L.; Hitchcock, A. P.; Scholl A.; Doran, A. *J. El. Spect. Rel. Phen.* In press 2008, doi:10.1016/j.elspec.2008.01.002.

(12) Rightor, E. G.; Hitchcock, A. P.; Ade, H.; Leapman, R. D.; Urquhart, S. G.; Smith, A. P.; Mitchell, G.; Fischer, D.; Shin, H. J.; Warwick, T. *J. Phys. Chem. B* **1997**, *101*, 1950.

(13) Kaznacheyev, K.; Osanna, A.; Jacobsen, C.; Plashkevych, O.; Vahtras, O.; Agren, H. *J. Phys. Chem. B* **2002**, *106*, 3153.

(14) Gordon, M. L.; Cooper, G.; Morin, C.; Araki, T.; Turci, C. C.; Kaznatcheev, K.; Hitchcock, A. P. *J. Phys. Chem. A* **2003**, *107*, 6144.

(15) Cooper, G.; Gordon, M.; Tulumello, D.; Turci, C.; Kaznatcheev, K.; Hitchcock, A. R. *J. El. Spect. Rel. Phen.* **2004**, *137*−*40*, 795.

(16) Zubavichus, Y.; Zharnikov, M.; Schaporenko, A.; Grunze, M. *J. El. Spect. Rel. Phen.* **2004**, *134*, 25.

(17) Zubavichus, Y.; Shaporenko, A.; Grunze, M.; Zharnikov, M. *J. Phys. Chem. A* **2005**, *109*, 6998.

(18) Zubavichus, Y.; Shaporenko, A.; Grunze, M.; Zharnikov, M. *J. Phys. Chem. B* **2006**, *110*, 3420.

(19) (a) Hermann, K.; Pettersson, L. G. M.; Casida, M. E.; Daul, C.; Goursot, A.; Koester, A.; Proynov, E.; St-Amant, A.; Salahub., D. R.;Contributing Authors. (b) Carravetta, V.; Godbout, N.; Guan, J.; Jamorski, C.; Leboeuf, M.; Malkin, V.; Malkina, O.; Nyberg, N.; Pedocchi, L.; Sim, F.; Triguero, L.; Vela, A. *StoBe Software*, StoBe-demon version 2.1, (2005).

(20) Nyberg, M.; Hasselström, J.; Karis, O.; Wassdahl, N.; Weinelt, M.; Nilsson, A.; Pettersson, L. G. M. *J. Chem. Phys.* **2000**, *112*, 5420.

(21) Nyberg, M.; Odelius, M.; Nilsson, A.; Pettersson, L. G. M. *J. Chem. Phys.* **2003**, *119*, 12577.

(22) Hasselström, J.; Karis, O.; Nyberg, M.; Pettersson, L. G. M.; Weinelt, M.; Wassdahl, N.; Nilsson, A. *J. Phys. Chem. B* **2000**, *104*, 11480.

(23) Hasselström, J.; Karis, O.; Weinelt, M.; Wassdahl, N.; Nilsson, A.; Nyberg, M.; Pettersson, L. G. M.; Samant, M. G.; Stöhr, J. *Surf. Sci.* **1998**, *407*, 221.

(24) Plashkevych, O.; Carravetta, V.; Vahtras, O.; Agren, H. *Chem. Phys.* **1998**, *232*, 49.

(25) Huzinaga, S.; Andzelm, J.; Klobukowski, M.; Radzio-Andzelm, E.; Sakai, Y.; Tatewaki, H. *Gaussian Basis Sets for Molecular Calculations*; Elsevier: Amsterdam, 1984.

(26) Hermann, K.; Pettersson, L. Documentation for *StoBe2005*, version 2.1, 2005.

(27) Kutzelnigg, W.; Fleischer, U.; Shindler, M. In *NMR-Basic Principles and Progress*; Springer-Verlag: New York, 1990; *23*, 165.

(28) Langan, P.; Mason, S. A.; Myles, D.; Schoenborn, B. P. *Act. Crystallogr.* **2002**, *B58*, 728.

(29) Cavalleri, M.; Odelius, M.; Nordlund, D.; Nilsson, A.; Pettersson, L. G. M. *Phys. Chem. Chem. Phys.* **2005**, *7*, 2854.

(30) George, G. N. *EXAFSPAK*: A Suite of Programs for Analysis of X-ray Absorption Spectra, 2000.

(31) Aziz, E. F.; Gråsjö, J.; Forsberg, J.; Andersson, E.; Söderström, J.; Duda, L.; Zhang, W.; Yang, J.; Eisebitt, S.; Bergström, C.; Luo, Y.; Nordgren, J.; Eberhardt, W.; Rubensson, J. E. *J. Phys. Chem. A* **2007**, *111*, 9662.

(32) Gillespie, A. W.; Walley, F. L.; Farrell, R. E.; Regier, T.; Blyth, R. I. R. *J. Synch. Rad.* **2008**, *15*, 532.

JP900794V